Journal of Materials Chemistry A

Accepted Manuscript

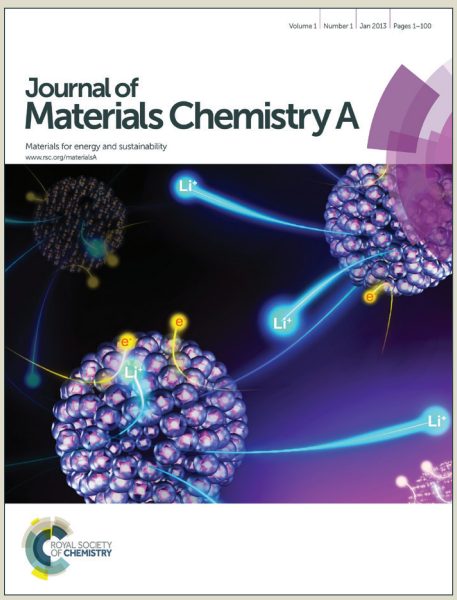

ROYAL SOCIETY OF CHEMISTRY

www.rsc.org/materialsA

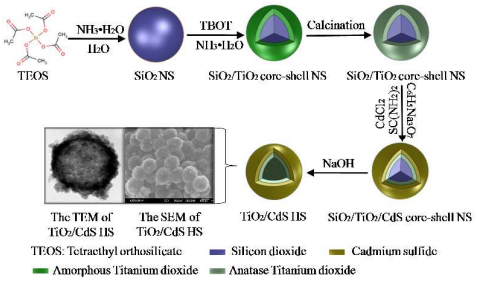

A sonochemical method has been devloped to fabricate hierarchical TiO_2/CdS hollow sphere heterostructures with excellent photocatalytic activity.

Journal of Materials Chemistry A

Cite this: DOI: 10.1039/c0xx00000x

www.rsc.org/xxxxxx

COMMUNICATION

A facile strategy for the synthesis of hierarchical TiO_2/CdS hollow sphere heterostructures with excellent visible light activity

Chao Xue,[a] Ting Wang,[a] Guidong Yang,*[a] Bolun Yang,[a] and Shujiang Ding,*[b]

Received (in XXX, XXX) Xth XXXXXXXXX 20XX, Accepted Xth XXXXXXXXX 20XX
DOI: 10.1039/b000000x

A facile and efficient strategy for the synthesis of hierarchical TiO_2/CdS hollow sphere (HS) heterostructures has been developed. Evaluation of the TiO_2/CdS HS heterostructures for the degradation of rhodamine B (RhB) and methyl orange (MO) revealed that they exhibit excellent photocatalytic activity under visible light irradiation.

Over the past decades, nanostructured titanium dioxide (TiO_2) have been intensively investigated as a n-type semiconductor photocatalytic material which has been widely used in industrial production such as photocatalysis, solar cells, bactericidal agents and self-cleaning technologies.[1-3] They ascribed these various applications to its low cost, high catalytic activity and nontoxicity.[4-7] Besides, it has been established that the structure of the photocatalyst surface plays a very important role for selectivity and photocatalytic activity in which most catalysis is carried out when the reactants are adsorbed onto the catalyst surface. Meanwhile, in order to enhance its specific surface area and catalytic activity, many controllable synthesis efforts have already been made to synthesize particles with well-defined sizes and shapes, such as monodisperse nanoparticles, hierarchical microspheres, hollow spheres, nanorods, nanotubes and porous network, *etc*.[8-12] Among these nanostructures, TiO_2 hollow sphere, a special core-shell nanostructures, have attracted increasing interest to researchers due to its properties of low density, large surface area, surface permeability, *etc*.[13-15]

However, as a wide bandgap semiconductor (Eg = 3.2 eV for anatase phase), TiO_2 HS can only be excited under UV irradiation with a wavelength shorter than 387 nm. And another major limiting factor is the high recombination rate of the photogenerated electron-hole pairs.[1] Therefore, an effective method have been pursued to extend the response of photocatalysts into visible-light region and improve the photocatalytic performance of TiO_2 nanostructures by combining with some narrow band gap semiconductors, for instance cadmium sulfide (CdS), so that it can be responsive to the solar spectrum.[13,16-18] It's well known that CdS is an intrinsic semiconductor with a narrow band gap of 2.42 eV which could be excited by visible light to produce electrons and holes.[2] Previous studies have shown that in TiO_2/CdS coupled system, heterojunctions between TiO_2 and coupled CdS nanoparticles have been formed and the conduction band (CB) of CdS is about 0.5 eV more negative than that of TiO_2. In other words, TiO_2 facilitates photoinduced charge transfer. Under visible light irradiation, the extra photogenerated electrons produced by the valence band (VB) of CdS transfer to the CB of TiO_2. Simultaneity, there are no any holes generated in the CB of TiO_2 and thus the recombination between electrons and holes was inhibited in the TiO_2/CdS composite. As a result, this coupled system can induce a large light-harvesting efficiency and supply more reaction active sites to improve the photocatalytic performance of the catalyst.

Up to now, a large number of techniques have been reported to combine TiO_2 with CdS, for instance, electrochemical deposition, spray pyrolysis deposition, successive ionic layer adsorption reaction and solvothermal method.[19,20] In spite of these efforts, the hierarchical TiO_2/CdS HS heterostructures prepared by the sonochemical method at a considerably low temperature was rarely reported. In this communication, a novel sonochemical method was designed to couple with CdS on the surface of SiO_2/TiO_2 core-shell nanospheres (see ESI for detail †).[14,21] In the process of coupling, different ammonia contents were taken into account which directly influence to the contents of S^{2-} ion participated in the reaction, and the resulting hierarchical TiO_2/CdS HS prepared with 1.75 mL and 2.0 mL of ammonia were denoted as D-B and E-B, respectively.

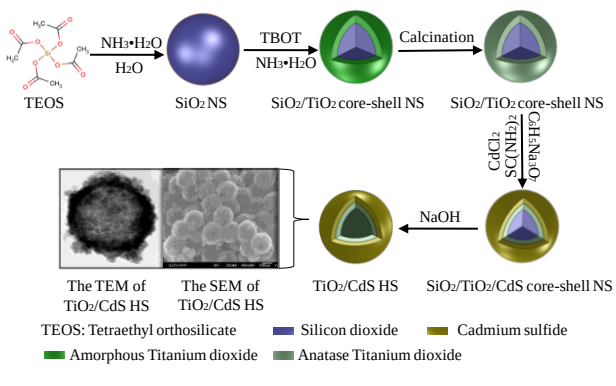

Fig. 1 Schematic diagram illustrating the synthetic route of TiO_2/CdS hollow sphere heterostructures.

The overall procedure for fabricating TiO_2/CdS HS heterostructures is schematically illustrated in Fig.1. SiO_2 nanospheres capped with TiO_2 and CdS were synthesized by a versatile multistep route. Firstly, SiO_2 nanospheres (NS) have been prepared from the catalytic hydrolysis of tetraethoxysilicate (TEOS) using modified Stöber method.[22] Under the condition of the ammonia catalysis, the hydrolysis reaction of TEOS has some advantages, such as a faster rate of hydrolysis and thoroughly hydrolyzate, *etc*.. These were favorable for the formation of

monodisperse silica spheres. Next, nanocrystalline TiO_2 interlayer was coated on the surface of SiO_2 core by the hydrolysis of tetra-n-butyl titanate (TBOT) in deionized water under vigorously stirring. Furthermore, the sonochemical method was then used to prepare CdS deposited on SiO_2/TiO_2 core-shell nanospheres. With the irradiation of ultrasound, ammonia of solution hydrolysis to produce -OH which would react with thiourea and therefore release S^{2-} ions, the interaction between S^{2-} ions and free Cd^{2+} ions in the solution was then occurred and continually formed CdS nanoparticles on the surface of SiO_2/TiO_2 core-shell nanospheres.[23] Finally, the innermost SiO_2 nanospheres were corrupted by a certain concentration of NaOH solution, in which the hierarchical TiO_2/CdS HS heterostructures were formed.

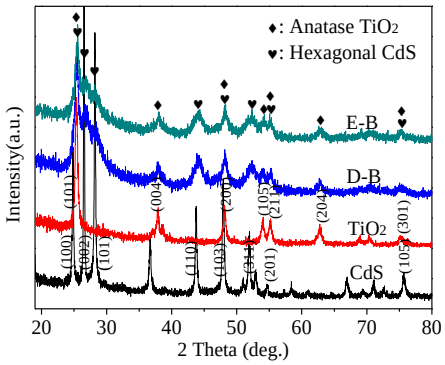

Fig. 2 X-ray diffraction patterns of the samples D-B, E-B together with the pure CdS and TiO_2.

Fig. 2 shows the XRD patterns of TiO_2/CdS HS heterostructures together with those of the pure CdS and TiO_2. The as-prepared D-B and E-B samples exhibit similar X-ray diffraction patterns, and the peaks at 2θ values of 24.83°, 26.52°, 28.21°, 43.77°, 47.93°, 51.95°, 54.74° and 75.58° were in good agreement with the (100), (002), (101), (110), (103), (311), (201) and (105) crystal planes of hexagonal structure CdS (JCPDS No. 65-3414), respectively.[24] In addition, the diffraction peaks at 37.80°, 53.89° and 62.69° in the XRD pattern of TiO_2/CdS HS can be attributed to the (004), (105) and (204) crystal planes of anatase TiO_2 (JCPDS No. 21-1272), respectively.[25] Besides, four distinct diffraction peaks observed at 25.28°, 48.05°, 55.06° and 76.02° in the D-B and E-B samples, corresponding to the (101), (200), (211) and (301) crystal planes of anatase TiO_2, can be found overlapping with (100), (103), (201) and (105) crystal planes of hexagonal CdS, respectively, owing to the positions of these peaks are quite similar. All the XRD patterns of TiO_2/CdS HS samples exhibit diffraction peaks corresponding to both anatase TiO_2 and hexagonal CdS, and no other impure peaks can be observed, suggesting a two-phase composition of TiO_2 and CdS in these heterostructures. Furthermore, the composition and functional groups of TiO_2/CdS HS heterostructures composites were further characterized by FT-IR spectroscopy (Fig. S1, ESI †), and the average crystallite size of the CdS and TiO_2 composite nanoparticles were also calculated from the peak width of the (002) plane of hexagonal CdS and the (101) plane of anatase TiO_2 by Scherrer's formula,[26] and these details can be observed in Table S1(ESI †).

Fig. 3 shows the typical SEM images of the hierarchical TiO_2/CdS HS resulting from the coating of TiO_2 and CdS onto the SiO_2 nanospheres. As shown in Fig. 3, some spheres (*i.e.*, W1) were complete, yet others (*i.e.*, B1) were broken, which demonstrate the formation of hollow structures. After capping TiO_2 and CdS, the quite smooth surface of the SiO_2 nanospheres (Fig. S2, ESI †) became relatively rough with an average diameter of 300 nm (shown in Fig. 4(b)), indicating that the successful fabrication of the hybrid nanostructures. The same statement can be obtained from the data of Energy Dispersive X-ray Spectrum (EDX, Fig. S3, ESI †), which shows that the as-prepared samples contain O, Ti, as well as S and Cd. The contents of CdS calculated according the atomic concentration was about 4.15% and 6.17% for D-B and E-B samples, respectively.

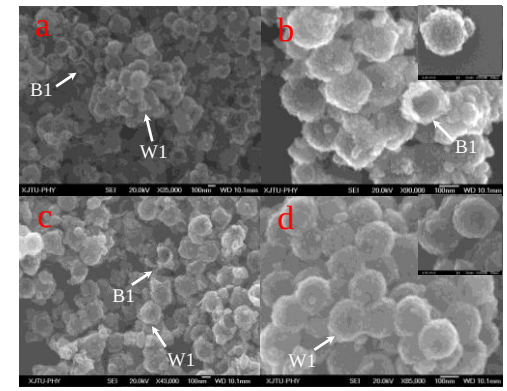

Fig. 3 SEM images(a-d) of the hierarchical TiO_2/CdS HS samples with various magnifications: (a and b) D-B sample, (c and d) E-B sample.

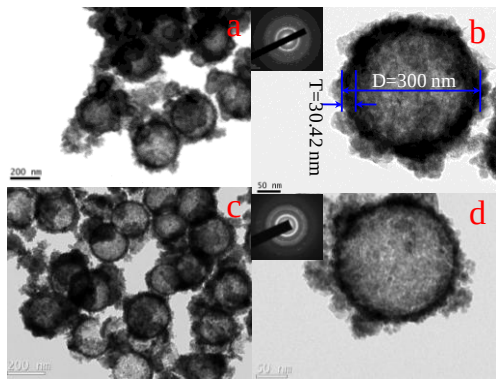

Fig. 4 TEM images (a-d) pattern of as-prepared samples: (a and b) D-B sample, (c and d) E-B sample.

The TEM images (Fig. 4) further verify that the as-prepared samples were the hierarchical TiO_2/CdS HS heterostructures in which different color contrast can be seen obviously between the central and fringe region of the spheres. As shown in Fig. 4(b), the thickness of TiO_2 shells is about 30 nm and interstitial voids about 237 nm in diameter. This value agreed well with the SEM observations. Furthermore, the selected area electron diffraction (SAED) patterns (inset of Fig. 4(b and d)) of the hierarchical TiO_2/CdS HS illustrate that the crystalline structure can be indexed to the expected crystal lattice of CdS and TiO_2. In addition, the HR-TEM image (Fig. S4, ESI †) revealed that the lattice spacings of the hierarchical TiO_2/CdS HS were 0.335 nm and 0.352 nm which correspond to the (002) plane of hexagonal CdS and the (101) plane of anatase TiO_2, respectively. It further confirmed the interfacial junction between CdS and TiO_2 in which CdS was closely attached on the surface of TiO_2 shells.

As shown in Fig. 5(a), the nitrogen adsorption-desorption isotherms of both D-B and E-B were similar and all of them were type-IV with hysteresis loops according to the IUPAC classification,[11] indicating that the presence of well-developed mesoporosity structure. In addition, an obvious absorption hysteresis loop located at $0.33< P/P_o< 0.99$ with a flat "S"-shape was observed in the isotherms of D-B and E-B, which could be categorized as type-H3 hysteresis loop, suggesting the existence of slit-like pores.[11,19] The BET surface area, pore volume and average pore sizes of two samples were summarized in Table S1 (ESI †). As calculated by the Brunauer-Emmett-Teller (BET)

method, such the hierarchical TiO_2/CdS HS (D-B) gives rise to a

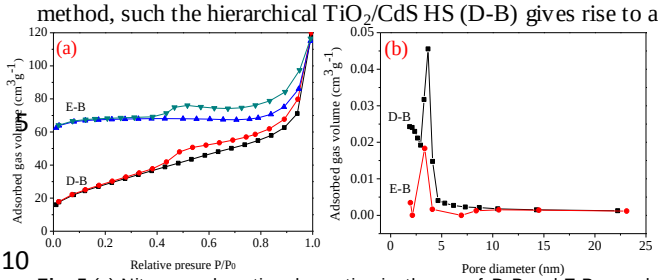

Fig. 5 (a) Nitrogen adsorption-desorption isotherms of D-B and E-B samples; (b) the corresponding pore size distributions curve of the hierarchical TiO_2/CdS HS.

BET surface area of 104.48 m^2/g and a relatively large pore volume of 0.18 cm^3/g, compared with 90.04 m^2/g and 0.12 cm^3/g for the E-B sample. It can be seen from the Fig. 5(b) that the pore size analysis from the adsorption branch of both samples exhibited similar narrow pore size distributions ranging from 2.13 nm to 4.74 nm. However, the average pore size (7.04 nm) of the D-B sample was larger than that of the E-B sample which was 5.29 nm. As well known, the hierarchical TiO_2/CdS HS occupied a large surface area, which could supply more reaction active sites and effectively promote the separation efficiency of the electron-hole pairs, resulting in a higher quantum efficiency of photocatalytic reaction. Meanwhile, the hollow sphere structures and its big specific surface area would reduce multiple scattering, leading to the improvement of the light harvesting.[27,28]

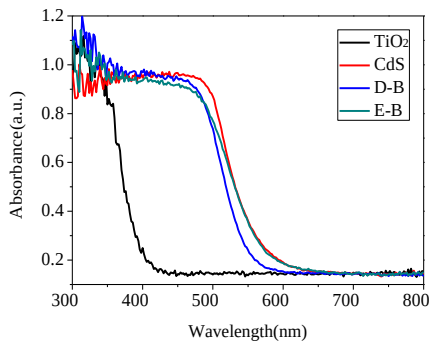

Fig. 6 UV-vis diffuse reflection spectra for samples D-B, E-B, pure CdS and TiO_2.

To investigate the optical properties, the UV-vis absorption spectra of hierarchical TiO_2/CdS HS samples with different ammonia amounts together with those of pure TiO_2 and CdS as comparison were shown in Fig. 6. It has been observed that the pure TiO_2 exhibits photoresponse in the UV region with a wavelength below 388 nm due to its big energy band gap (3.2eV).[15] In comparison with pure TiO_2, the absorption edge of D-B and E-B samples were drastically extended to around 555 nm and 575 nm, respectively. It's well known that CdS has a narrow energy band gap and thus exhibits better visible light response ability. The expansion of absorption edge of the hierarchical TiO_2/CdS HS heterostructures was mainly resulted from the photosensitization of CdS rather than the formation of discrete energy levels.[29-31] Moreover, the light absorption edge of D-B sample showed a bit narrower than that of the pure CdS and E-B which extended to approximately 575 nm. The causes of this phenomenon might be attributed to the stronger combination and more uniform heterojunctions between CdS and TiO_2 crystallites. According to the relevant literature, within a certain range, the photosensitizing effect of CdS could be improved with the gradually increasing of the amount of CdS, consequently, resulting in the expansion of visible light absorption range. In this work, since the coupling amount of CdS in D-B sample was less than that in E-B sample and pure CdS, as a result of leading to the poor photosensitization of CdS in D-B sample.[29] Furthermore, quantum-size effect also has certain influence on the expansion of the light absorption range. With the decreasing of the particle size, the absorption of CdS quantum dots appears obvious blue shift. Obviously, after coupling with anatase TiO_2, the crystal size of hexagonal CdS in D-B sample was calculated to be 17.98 nm, which was smaller than that of E-B sample (about 28.04 nm) and pure CdS (about 26.52 nm) (Table S1, ESI †). The absorption band of D-B sample was blue shifted probably resulting from the size quantization effects in D-B sample.[26,32-35]

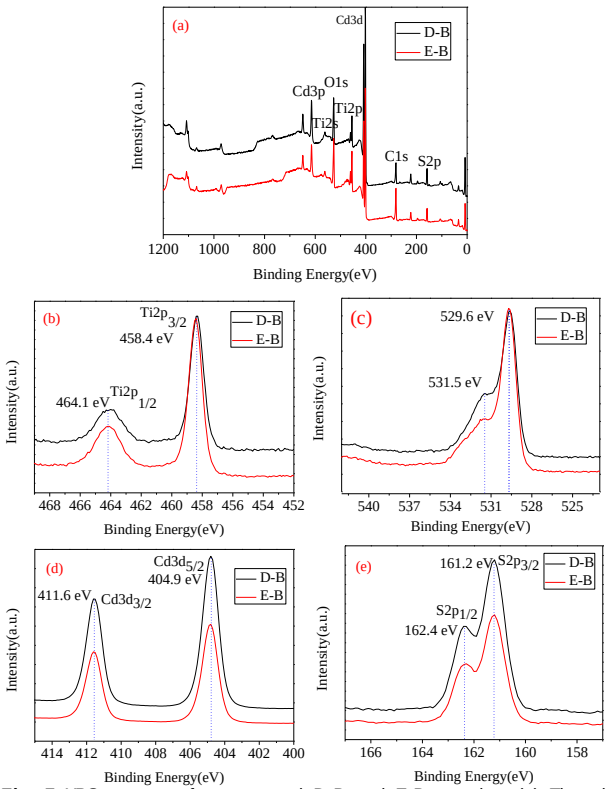

Fig. 7 XPS spectra of as-prepared D-B and E-B samples. (a) The whole survey spectrum; (b) Ti 2p XPS spectrum; (c) O1s XPS spectrum; (d) Cd 3d XPS spectrum and (e) S 2p XPS spectrum.

The X-ray photoelectron spectroscopy (XPS) was performed to further investigate the elemental composition and surface chemical state of the obtained hierarchical TiO_2/CdS HS samples. As depicted in the whole XPS survey spectrum (Fig. 7(a)), the elemental composition on the surface of as-prepared D-B and E-B samples can be found to be S, C, Cd, Ti and O elements, which correspond to the values of the binding energy 162.3 eV, 284.6 eV, 404.8 eV, 458.4 eV and 531.4 eV, respectively.[16,36,37] The XPS spectrum for the C1s peak might be attributed to the adventitious carbonaceous species formed in the process of preparation. The high-resolution XPS spectra of the Ti 2p region on the surface of the obtained hierarchical TiO_2/CdS HS samples were shown in Fig. 7(b). The binding energies of Ti $2p_{3/2}$ and Ti $2p_{1/2}$ in those samples were 458.4 eV and 464.1 eV, respectively, which was a characteristic of Ti^{4+} on the surface of the hierarchical TiO_2/CdS HS.[38] O 1s XPS spectra were shown in Fig. 7(c), in which the two asymmetric peaks centered at 529.6 eV and 531.5 eV were associated with the lattice oxygen of TiO_2 and the surface adsorbed components of hydroxyl group (-OH), respectively.[39,40] As shown in Fig. 7(d), two sharp peaks observed at binding energies of 411.6 eV and 404.9 eV can be assigned to the characteristic of Cd $3d_{3/2}$ and Cd $3d_{5/2}$, respectively. Furthermore, a spin-orbit separation of 6.7 eV between Cd $3d_{3/2}$ and Cd $3d_{5/2}$

further confirmed the existence of Cd^{2+} on the surface of the hierarchical TiO_2/CdS HS samples.[41] Fig. 7(e) intuitively demonstrates the S 2p XPS spectrum of as-prepared D-B and E-B samples. The double peaks located at 161.2 eV and 162.4 eV could be attributed to the characteristic doublets of S $2p_{3/2}$ and S $2p_{1/2}$, which indicated that the chemical state of S element mainly in the form of S^{2-} exists on the surface of hierarchical TiO_2/CdS HS samples. In a word, the XPS results further proved that the co-existence of CdS and TiO_2 in the hierarchical TiO_2/CdS HS.

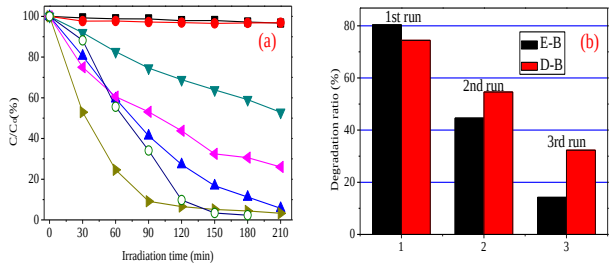

Fig. 8 (a) Plots of the decomposition of RhB solution concentration versus irradiation time by different samples under visible-light irradiation (λ≥420 nm), RhB (■), commercial TiO_2(●), P25 TiO_2 (▲), SiO_2/TiO_2(▼), CdS(◀), E-B(▶) and D-B(○). The original concentration of RhB solution is 15 mg/L. (b) Recycling tests of RhB photodegradation on D-B and E-B samples under visible light irradiation for 90 min.

The photocatalytic activity of the hierarchical TiO_2/CdS HS has been evaluated by using the RhB solution of 15mg/L as the model pollutant under visible light irradiation and ambient conditions. For comparison, the photocatalytic activities of pure commercial TiO_2, P25 TiO_2, CdS and SiO_2/TiO_2 as well as without photocatalyst (the blank test) were also tested in the same system. As depicted in Fig. 8(a), the degradation of RhB by the pure commercial TiO_2 and the blank test were almost negligible after 210 min of visible light irradiation. Although commercial P25 TiO_2 and SiO_2/TiO_2 could not respond to visible light, RhB could also be decomposed by the two samples and the degradation efficiencies reached to 72.8% for P25 TiO_2 and 30.7% for SiO_2/TiO_2, respectively, after 120 min photoreaction. The causes of the phenomenon could be attributed to the photosensitization mechanism of RhB. It was worth noting that the different photocatalytic activity between commercial P25 TiO_2 and SiO_2/TiO_2 might be caused by two aspects: On the one hand, the commercial P25 TiO_2 particles were composed by two kinds of crystal shape: anatase and rutile TiO_2.[17] On the other hand, under the same photocatalytic reaction conditions, the quantity of TiO_2 in the SiO_2/TiO_2 catalyst is less than that of P25 TiO_2. Also, after 120 min visible light irradiation, more than 57.2% and 90.5% of RhB could be degraded in the presence of pure CdS and D-B sample, respectively. In contrast, the E-B sample exhibited a silghtly higher photocatalytic activity than D-B sample, and the degradation efficiencies was about 94.2% within 120 min visible light irradiation. As shown in Fig. S5 (ESI †), the trend that the absorption peak blue-shifts and broadens caused by de-ethylation of RhB also depicted the concentration diminution of RhB with increasing irradiation time.[28]

Fig. S6 (ESI †) shows the results of the photodegradation of MO solution by the as-synthesized catalysts, which further confirmed that the hierarchical TiO_2/CdS HS samples possess good photocatalytic performance under visible light irradiation. Interestingly, the P25 TiO_2 sample almost shows no MO degradation ability because the MO is more stable and possesses lower photosensitization. Furthermore, the photocatalytic activity of the resulting hierarchical TiO_2/CdS HS prepared with different ammonia amount was also tested, and the results were shown in Fig. S7, (ESI †). It can be seen that the varying amount of ammonia have obvious effect on the photocatalytic activity of photocatalysts, the E-B sample shows the highest activity among the four hierarchical TiO_2/CdS HS samples. In short, the improvement of visible-light adsorption, larger surface area, the synergic effect within the heterojunctions between CdS and TiO_2 crystallites and the unique morphologies and nanostructures of the hierarchical HS were supposed to be responsible for the efficient charge separation and the highly efficient photocatalytic activity of the hierarchical TiO_2/CdS HS.[26-29,42]

In order to investigate the stability and recyclability of the as-prepared hierarchical TiO_2/CdS HS, recycling tests of the visible-light-driven photodegradation activity of RhB were performed for certain times on the recycled D-B and E-B samples. As shown in Fig. 8(b), in the first round of illumination, D-B and E-B samples exhibited excellent visible light photocatalytic activity for RhB and the degradation ratio up to 74.5% and 80.4%, respectively. As can be seen that, from the second recycling test experiment, the recycled D-B sample showed higher stability and recyclability as well as the catalytic activity than that of E-B during the per decolorized reaction. However, after three runs of photodegradation of RhB, both D-B and E-B samples were partially lost their photocatalytic activity and the degradation efficiency only amounts to 32.33% and 14.20%, respectively, within 90 min visible light reaction. During the cycling tests, the photocorrosion reaction of CdS and the catalyst mass loss account for the gradual decrease of photocatalytic activity.[15,16,43-45] Therefore, how to improve the stability and photocatalytic properties of hierarchical TiO_2/CdS HS materials become the focus of our next research.

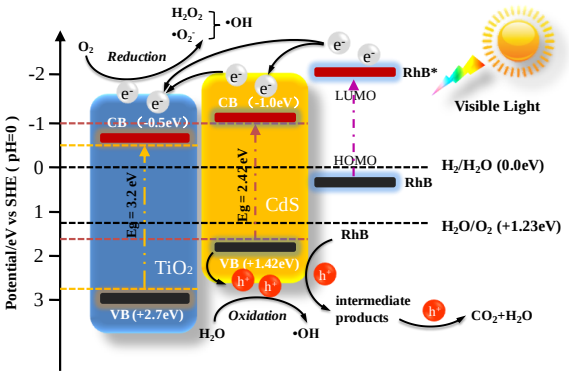

Fig. 9 Scheme illustrating the principle of charge-transfer and the photocatalytic processes on the interface of the hierarchical TiO_2/CdS HS under visible light irradiation.

Based on the above discussion, the as-prepared hierarchical TiO_2/CdS HS showed the excellent photocatalytic performance in the degradation of organic compounds, such as RhB. The degradation mechanism of organic pollutants over the hierarchical TiO_2/CdS HS was further explored and schematically illustrated in Fig. 9. Under the excitation of visible light, charge carriers were produced on the semiconductor of CdS due to its narrow energy band gap of 2.42 eV and then the photo-excited electron on the VB of CdS can be promoted to the CB of itself. It's well known that the CB of anatase TiO_2 was about 0.5 eV more positive than the bands of CdS. This matchable energy band position and intimate interfacial contact between CdS and TiO_2 facilitated a readily transfer of photo-excited electrons to the CB of anatase TiO_2 away from the CB of CdS while holes were still stranded in the surface of CdS nanoparticles. As a result, the recombination between electrons and holes was subsequently suppressed, allowing more opportunities for electrons and holes to participate in the oxidation-reduction reactions. On the one hand, the electrons would be trapped by adsorbed O_2 to form superoxide radical ($\bullet O_2^-$) and hydrogen peroxide (H_2O_2),[46] and then the two substances would work together to create a new

active species, namely the hydroxyl radical (•OH) which was very strong oxidants capable of effectively decomposing RhB. On the other hand, *in situ* generated holes in CdS could directly oxidize RhB molecules which adsorbed on the surface of the hierarchical TiO_2/CdS HS heterostructures. Moreover, because the E_{VB} of CdS (+1.42 eV vs. SHE) was more positive than $E(H_2O/O_2)$ (+1.23 eV vs. SHE), if organic pollutants adsorption was insignificant, the holes might react with H_2O adsorbed on surface of the photocatalyst, and generate hydroxyl radical (•OH), which simultaneously assisted in the decomposition of organic substances.[19,23,36,47] Hence, we believed that because of the synergistic effects between the generation of hydroxyl radical and holes, the TiO_2/CdS HS show the enhanced visible light catalytic activity for RhB degradation.

In addition to the synergy of the •OH and holes, the RhB may be excited by visible light irradiation due to the photosensitization, and which also contributes to the higher activity. As depicted in Fig. 9, under the excitation of visible light, the electrons on the LUMO level of the photoexcited RhB dye (RhB*) were generated and rapidly injected into the CB of CdS or TiO_2.[48,49] Meanwhile, RhB dye was converted to the cationic dye radical ($RhB^{\bullet+}$),[26] which might be reduced by superoxide radical ($\bullet O_2^-$), transformed and decomposed into intermediate products and finally mineralized to CO_2 and H_2O. However, the photocatalytic reaction mentioned above would not become the dominant factor because of the interaction between superoxide radical ($\bullet O_2^-$) and hydrogen peroxide (H_2O_2).[50]

Conclusions

In summary, we have successfully synthesized the hierarchical TiO_2/CdS HS by a novel sonochemical method. E-B sample exhibited a higher photocatalytic activity for degrading RhB under the excitation of visible light than D-B sample. The as-prepared hierarchical TiO_2/CdS HS occupy good light-absorption ability, superior surface properties and favourable photogenerated charge-separation efficiency which might have promising applications in the cleanup of environment.

Acknowledgements

This work was financially supported by the National Natural Science Foundation of China (Grant No. 21303130), and the Fundamental Research Funds for the Central Universities (Grant No. 2012jdhz40).

Notes and references

[a] *Department of Chemical Engineering, School of Chemical Engineering and Technology, Xi'an Jiaotong University, Xi'an, 710049, China. Fax: (+86) 29-8266-3189; E-mail: guidongyang@mail.xjtu.edu.cn*

[b] *Department of Applied Chemistry, School of Science, Xi'an Jiaotong University, Xi'an, 710049, China. E-mail: dingsj@mail.xjtu.edu.cn*

† Electronic Supplementary Information (ESI) available: Experimental procedure, FT-IR spectra, SEM image, EDX spectrum, Structure parameters, HR-TEM image, Photocatalytic activity and UV-vis spectral. See DOI: 10.103 9/b000000x/

1 G. Yang, T. Wang, B. Yang, Z. Yan, S. Ding, T. Xiao, *Appl. Surf. Sci.*, 2013, **285**, 135.
2 R. Pan, Y. Wu and K. Liew, *Appl. Surf. Sci.*, 2010, **256**, 6564-6568.
3 H. U. Lee, S. C. Lee, S. Choi, B. Son, H. Kim, S. M. Lee, H. J. Kim and J. Lee, *J. Hazard. Mater.*, 2013, **258**, 10-18.
4 G. Yang, Z. Yan, T. Xiao, B. Yang, *J. Alloys Compd.*, 2013, **580**, 15.
5 C.-W. Wang, J.-B. Chen, L.-Q. Wang, Y.-M. Kang, D.-S. Li and F. Zhou, *Thin Solid Films*, 2012, **520**, 5036.
6 L. Zhang, V. M.-Flores, N. Murakami and T. Ohno, *Appl. Surf. Sci.*, 2012, **258**, 5803.
7 M. Hoffmann, S. Martin, W. Choi and D. Bahnemann, *Chem. Rev.*, 1995, **95**, 70.
8 L. Yu, Z. Wang, L. Zhang, H. B. Wu and X. W. Lou, *J. Mater. Chem., A*, 2013, **1**, 122.
9 Q. Zhang, I. Lee, J. B. Joo, F. Zaera and Y. Yin, *Acc. Chem. Res.*, 2013, **46**,1816.
10 S. Kang, D. Yin, X. Li, L. Liang and J. Mu, *Mater. Res. Bull.*, 2012, **47**, 3065.
11 J. Zhang, Y. Wang, J. Jin, J. Zhang, Z. Lin, F. Huang and J. Yu, *ACS Appl. Mater. Interfaces*, 2013, **5**, 10317-10324.
12 A. Pan, H. B. Wu, L. Yu and X. W. Lou, *Angew. Chem. Int. Ed.*, 2013, **125**, 2282.
13 H. Meng, C. Cui, H. Shen, D. Liang, Y. Xue, P. Li and W. Tang , *J. Alloys Compd.*, 2012, **527**, 30.
14 A. A. Rafati, A. R. A. Borujeni, M. Najafi and A. Bagheri, *Mater. Charact.*, 2011, **62**, 94.
15 G. Li, L. Wu, F. Li, P. Xu, D. Zhang and H. Li, *Nanoscale*, 2013, **5**, 2118-2125.
16 Y. Liu, L. Zhou, Y. Hu, C. Guo, H. Qian, F. Zhang and X. W. Lou, *J. Mater. Chem.*, 2011, **21**, 18359.
17 J. C. Kim, J. Choi, Y. B. Lee, J. H. Hong, J. I. Lee, J. W. Yang, W. I. Lee and N. H. Hur, *Chem. Commun.*, 2006, **48**, 5024.
18 M. Mrowetz, W. Balcerski, A. Colussi and M. Hoffmann, *J. Phys. Chem. B*, 2004, **108**, 17269-17273.
19 G. Yang, B. Yang, T. Xiao and Z. Yan, *Appl. Surf. Sci.*, 2013, **283**, 402-410.
20 F.-X. Xiao, J. Miao, H.-Y. Wang and B. Liu, *J. Mater. Chem. A*, 2013, **1**, 12230.
21 N. Ghows and M. Entezari, *Ultrason. Sonochem.*, 2012, **19**, 1071.
22 M. Nakamura and K. Ishimura, *Langmuir*, 2008, **24**, 5100.
23 F. Xu, Y. Yuan, H. Han, D. Wu, Z. Gao and Kai Jiang, *Cryst. Eng. Comm.*, 2012, **14**, 3618.
24 S. Liu, N. Zhang, Z.-R. Tang and Y.-J. Xu, *ACS Appl. Mater. Interfaces*, 2012, **4**, 6380.
25 S. Qian, C. Wang, W. Liu, Y. Zhu, W. Yao and X. Lu, *J. Mater. Chem.*, 2011, **21**, 4947.
26 J.-W. Shi, X. Yan, H.-J. Cui, X. Zong, M.-L. Fu, S. Chen and L. Wang, *J. Mol. Catal. A: Chem.*, 2012, **356**, 53-60.
27 B. Jiang, X. Yang, X. Li, D. Zhang, J. Zhu and G. Li, *J. Sol-Gel Sci. Technol.*, 2013, **66**, 506-508.
28 H. Li, Z. Bian, J. Zhu, D. Zhang, G. Li, Y. Huo, H. Li and Y. Lu, *J. Amer. Chem. Soc.*, 2007, **129**, 8407.
29 Y. Huo, X. Yang, J. Zhu and H. Li, *Appl. Catal. B: Environ.*, 2011, **106**, 73.
30 K. Wu, H. Zhu, Z. Liu, W. R. Córdoba and T. Lian, *J. Am. Chem. Soc.*, 2012, **134**, 10337.
31 K. Tvrdy, P. A. Frantsuzov and P.V. Kamat, *PNAS*, 2011, **108**, 29-34.
32 S. Vaidya, A. Patra and A. K. Ganguli, *Colloids Surf., A: Physicochem. Eng. Aspects*, 2010, **363**,130-134.
33 I. Robel, V. Subramanian, M. Kuno and P.V. Kamat, *J. Am. Chem. Soc.*, 2006, **128**, 2385-2393.
34 V. Chakrapani, D. Baker and P. V. Kamat, *J. Am. Chem. Soc.*, 2011, **133**, 9607-9615.
35 Y. Yang, W. Rodr ́guez- Córdoba, X. Xiang and T. Lian, *Nano Lett.*, 2012, **12**, 303-309.
36 S. Singh, H. Kaur, V. N. Singh, K. Jain and T. D. Senguttuvan, *Sens. Actuators, B*, 2012,**171**, 901.
37 S. Ding, X. Yin, X. L ü, Y. Wang, F. Huang and D. Wan, *ACS Appl. Mater. Interfaces*, 2012, **4**, 308.
38 Y. C. Zhang, J. Li and H. Y. Xu, *Appl. Catal. B: Environ.*, 2012, **123**, 20.
39 G. Yang, Z. Yan, T. Xiao, *Appl. Surf. Sci.*, 2012, **258**, 8708.
40 K. Yu, S. Yang, H. He, C. Sun, C. Gu and Y. Ju, *J. Phys. Chem. A*, 2009, **113**, 10024-10032.
41 L. Wu, J. C. Yu and X. Fu, *J. Mol. Catal. A: Chem.*, 2006, **244**, 27.
42 J. S. Chen, J. Liu, S. Z. Qiao, R. Xu and X. W. Lou, *Chem. Commun.*, 2011, **47**, 10443-10445.
43 Y. Liu, L. Yu, Y. Hu, C. Guo, F. Zhang and X. W. Lou, *Nanoscale*, 2012, **4**, 186.
44 J. Fu, B. Chang, Y. Tian, F. Xi and X. Dong, *J. Mater. Chem. A*, 2013, **1**, 3083-3090.
45 J. S. Jang, S. H. Choi, H. G. Kim and J. S. Lee, *J. Phys. Chem. C*, 2008, **112**,17204.
46 B. Tian, T. Wang, R. Dong, S. Bao, F. Yang and J. Zhang, *Appl. Catal., B*, 2014, **147**, 27.
47 W. Z. Tang and C. P. Huang, *Water Res.*, 1995, **29**, 747.

48 A. Boulesbaa, A. Issac, D. Stockwell, Z. Huang, J. Huang, J. Guo and T. Lian, *J. Am. Chem. Soc.*, 2007, **129**, 15132-15133.
49 S. Jin and T. Lian, *Nano Lett.*, 2009, **9**, 2448-2454.
50 L. Kong, Z. Jiang, H. H. Lai, R. J. Nicholls, T. Xiao, M. O. Jones and Peter P. Edwards, *J. Catal.*, 2012, **293**, 118-119.